JYX
JYVÄSKYLÄN YLIOPISTO
UNIVERSITY OF JYVÄSKYLÄ

**This is a self-archived version of an original article. This version may differ from the original in pagination and typographic details.**

**Author(s):** Kujala, Jan; Ciumas, Carolina; Jung, Julien; Bouvard, Sandrine; Lecaignard, Françoise; Lothe, Amélie; Bouet, Romain; Ryvlin, Philippe; Jerbi, Karim

**Title:** GABAergic inhibition shapes behavior and neural dynamics in human visual working memory

**Year:** 2024

**Version:** Published version

**Copyright:** © 2024 the Authors

**Rights:** CC BY-NC 4.0

**Rights url:** https://creativecommons.org/licenses/by-nc/4.0/

**Please cite the original version:**

Kujala, J., Ciumas, C., Jung, J., Bouvard, S., Lecaignard, F., Lothe, A., Bouet, R., Ryvlin, P., & Jerbi, K. (2024). GABAergic inhibition shapes behavior and neural dynamics in human visual working memory. Cerebral Cortex, 34(2), Article bhad522. https://doi.org/10.1093/cercor/bhad522

OXFORD

*Cerebral Cortex*, 2024, 1–13
https://doi.org/10.1093/cercor/bhad522
**Original Article**

# GABAergic inhibition shapes behavior and neural dynamics in human visual working memory

Jan Kujala[1,2,*], Carolina Ciumas[2,3], Julien Jung[2,4], Sandrine Bouvard[3,5], Françoise Lecaignard[2,5], Amélie Lothe[2], Romain Bouet[2], Philippe Ryvlin[2,3,6], Karim Jerbi[2,7]

[1]Department of Psychology, University of Jyväskylä, PO Box 35, Jyvaskyla FI-40014, Finland,
[2]Lyon Neuroscience Research Center, INSERM U1028 - CNRS UMR5292, Lyon F-69000, France,
[3]Institute for Child and Adolescent with Epilepsy (IDEE), Lyon F-69000, France,
[4]Department of Epileptology and Functional Neurology, Lyon Neurological Hospital, Lyon F-69000, France,
[5]CERMEP Imaging Center, Bron F-69003, France,
[6]Department of Clinical Neurosciences, CHUV, Lausanne 1011, Switzerland,
[7]Department of Psychology, University of Montreal, Montreal, Québec H3C 3J7, Canada

*Corresponding author: Department of Psychology, University of Jyväskylä, PO Box 35, Jyvaskyla FI-40014, Finland. Email: jan.j.kujala@jyu.fi

Neuronal inhibition, primarily mediated by GABAergic neurotransmission, is crucial for brain development and healthy cognition. Gamma-aminobutyric acid concentration levels in sensory areas have been shown to correlate with hemodynamic and oscillatory neuronal responses. How these measures relate to one another during working memory, a higher-order cognitive process, is still poorly understood. We address this gap by collecting magnetoencephalography, functional magnetic resonance imaging, and Flumazenil positron emission tomography data within the same subject cohort using an n-back working-memory paradigm. By probing the relationship between $GABA_A$ receptor distribution, neural oscillations, and Blood Oxygen Level Dependent (BOLD) modulations, we found that $GABA_A$ receptor density in higher-order cortical areas predicted the reaction times on the working-memory task and correlated positively with the peak frequency of gamma power modulations and negatively with BOLD amplitude. These findings support and extend theories linking gamma oscillations and hemodynamic responses to gamma-aminobutyric acid neurotransmission and to the excitation-inhibition balance and cognitive performance in humans. Considering the small sample size of the study, future studies should test whether these findings also hold for other, larger cohorts as well as to examine in detail how the GABAergic system and neural fluctuations jointly support working-memory task performance.

*Key words*: functional magnetic resonance imaging; magnetoencephalography; n-back; neurotransmission; positron emission tomography.

## Introduction

A finely orchestrated balance between excitation and inhibition is central to healthy brain function. Distinct brain imaging techniques provide complementary insights into brain function by tapping into distinct physiological signatures of brain activity at multiple spatial and temporal scales. Despite important advances, our grasp on the neural bases of cognition remains arguably fragmented because the relationship between the findings obtained across different imaging modalities is not fully elucidated. In particular, how synaptic neurotransmission relates to electrophysiological and to hemodynamic responses is still largely unsettled. A handful of studies have sought to overcome this limitation by combining insights from multiple modalities, including methods that probe hemodynamic and electrophysiological (e.g. oscillatory) brain responses as well as gamma-aminobutyric acid (GABA) concentration (Muthukumaraswamy et al. 2009). However, previous work that has jointly probed these measures has focused essentially on primary sensory or motor areas (Muthukumaraswamy et al. 2009; Boy et al. 2010; Kujala et al. 2015) and it is unclear how these features relate to one another in the case of higher-order cognitive systems, such as working memory (WM). Harnessing such an understanding would be crucial to bridge findings and combine insights from various studies of the neural underpinnings of human cognition. The construction and neural underpinnings of WM have been studied extensively via, e.g. behavioral models (Baddeley 2003; Myers et al. 2017), hemodynamic (Owen et al. 2005) and electrophysiological neuroimaging (Palva et al. 2010; Roux and Uhlhaas 2014; Eriksson et al. 2015), stimulation based approaches (van de Ven et al. 2012) as well as neurotransmitter investigations (Michels et al. 2012; Yoon et al. 2016), also by combining two or more of these alternatives (Khursheed et al. 2011; Takei et al. 2016; Mederos et al. 2021). These studies have revealed distinct executive and storage components within WM as well as highlighted the role of a range of neural processes and cortical structures involved in efficient WM performance. However, because previous work on WM did not simultaneously examine hemodynamics, electrophysiology, and synaptic neurotransmission, the links between the insights

**Received:** July 13, 2023. **Revised:** December 8, 2023. **Accepted:** December 9, 2023
© The Author(s) 2024. Published by Oxford University Press.
This is an Open Access article distributed under the terms of the Creative Commons Attribution Non-Commercial License (https://creativecommons.org/licenses/by-nc/4.0/), which permits non-commercial re-use, distribution, and reproduction in any medium, provided the original work is properly cited. For commercial re-use, please contact journals.permissions@oup.com

Downloaded from https://academic.oup.com/cercor/advance-article/doi/10.1093/cercor/bhad522/7512628 by Jyvaskyla University user on 17 January 2024

afforded by these different signatures of WM have yet to be established.

The last 15 years have witnessed a rising interest in determining the links between GABAergic inhibition and both electrophysiological and hemodynamic signaling (Edden and Barker 2007; Northoff et al. 2007; Muthukumaraswamy et al. 2009; Cousijn et al. 2014; Kujala et al. 2015; Balz et al. 2016). However, only a few studies have sought to evaluate the relationship between GABAergic inhibition and other neural signals in higher order cortical regions (Takei et al. 2016). Despite the consensus that such multimodal studies are necessary, they are complex, costly and can be methodologically challenging given the diversity of expertise required. Incidentally, the wealth of research conducted on WM would particularly benefit from such systems-level insights in order to bridge observations from different imaging modalities (Schmidt-Wilcke et al. 2018).

Investigations applying electrophysiological approaches to WM have revealed that it builds on a wide range of oscillatory mechanisms (Palva et al. 2010, 2011; Roux et al. 2012; Roux and Uhlhaas 2014; Honkanen et al. 2015; Daume et al. 2017; Johnson et al. 2017; Popov et al. 2018; Carver et al. 2019) associated with different roles ranging from maintenance to inhibition and to the organization of items (Roux and Uhlhaas 2014), with the interactions between oscillations facilitating the functioning of the WM system as a whole (Alekseichuk et al. 2016; Johnson et al. 2017). In particular, electrophysiological studies have shown that oscillatory activity and bursting in the gamma band play a vital role in WM (Roux et al. 2012; Lundqvist et al. 2016) and that this activity is linked both to the subjects' memory capacity and to task accuracy (Palva et al. 2011; Honkanen et al. 2015). Functional magnetic resonance imaging (fMRI) studies, in turn, have revealed intricate patterns of brain areas in these regions supporting encoding, maintenance and retrieval of distinct features, object manipulation and inhibition of distracting stimuli (D'Esposito et al. 1999, 2000; Rahm et al. 2013; Cohen et al. 2014; Ester et al. 2015; Lara and Wallis 2015). Akin to electrophysiological investigations, fMRI-based studies have demonstrated that interactions between various neurocognitive components are central in WM performance, especially in demanding tasks (Diwadkar et al. 2000; Soreq et al. 2019). In recent years, magnetic resonance spectroscopy (MRS) studies have also shown that increased GABA levels and GABA-to-glutamate ratios are beneficial to WM capacity and accuracy (Yoon et al. 2016; Marsman et al. 2017; Ragland et al. 2020). These results along with evidence from receptor antagonist studies underline the importance of both glutamate and GABA in neuronal firing during WM tasks (Wang et al. 2013; Rodermund et al. 2020). Pharmacological manipulations have also been used to show that GABAergic interneurons play a key role in the generation of both alpha- and gamma-band oscillations which, in turn, link to WM performance (Lozano-Soldevilla et al. 2014). Moreover, MRS-based studies have demonstrated that both the frequency and amplitude of neural oscillations correlate with GABA concentration as well as WM performance (Takei et al. 2016).

However, because previous studies on WM have not simultaneously probed electrophysiological, hemodynamic, GABAergic and behavioral measures, bridging findings from the different streams of research on WM has remained a challenge, limiting progress toward a holistic understanding of the neural basis of WM. It is possible that the relationships between GABAergic, electrophysiological and hemodynamic signals that have been observed in sensory and motor areas comprise a general principle that holds also in higher-order cortical networks. However, there has been no evidence to date to support this.

Here, we address this gap by combining, for the first time, magnetoencephalography (MEG), fMRI, Flumazenil positron emission tomography (FMZ-PET) data and behavioral measures, recorded in the same subject cohort during a classical WM task. These rare, yet small-scale data with thirteen subjects, allow initial exploration of the joint role of the GABAergic system and neural and hemodynamic fluctuations in WM. More specifically, through this unique combination of modalities, and inspired by previous reports on the roles of gamma activity in both WM and neuronal inhibition, we probe the link between gamma oscillations, Blood Oxygen Level Dependent (BOLD) and $GABA_A$ receptor distribution in WM networks and we examine how these features relate to behavior. We expect that the $GABA_A$ receptor density in higher order cortical regions involved in WM would show positive correlations with gamma-band oscillatory frequency and negative correlations with BOLD amplitude. Moreover, we expect that across the neural measures particularly the $GABA_A$ receptor density is linked with WM task performance.

## Materials and methods

### Subjects and experimental design

Thirteen healthy, native French-speaking subjects participated in the study. fMRI data were collected successfully from all 13 subjects. For one subject, the MEG recording failed due to technical reasons and one subject did not participate in the PET recording. Moreover, the MEG data of one subject had to be discarded due to excessive blinking. Data of sufficient quality were recorded with all three modalities (PET, MEG, fMRI) from 10 subjects (1 female, 9 males; age 19–29 years, mean 24 years). All research was performed in accordance with the Declaration of Helsinki. Informed consent was obtained from all subjects, in agreement with the prior approval of the Institutional Review Board and by the National French Science Ethical Committee (CPPRB). All methods were conducted in accordance with the CPPRB guidelines. The fMRI and MEG experiments consisted of a classical WM task of visually presented letters, with 3 s intervals between consecutive letters. Each letter was shown for 300 ms. The paradigm comprised three different memory load conditions (1-back, 2-back, and 3-back tasks), and the subjects indicated with a button press, after each letter, whether the letter matched or did not match the appropriate preceding letter. In the fMRI experiment, we also collected resting-state data.

### Behavioral data analysis

The performance of the subjects in the WM tasks was estimated based on the MEG data that also contained the type (match/nonmatch) and timing of the subjects' responses. Here, we computed the number of correct and incorrect responses as well as separate reaction times for them within each individual and WM task. Trials for which the reaction times fell outside 2 standard deviations of the average within the task were excluded from the analyses. Based on the number of true/false positive/negative responses, we also derived the accuracy, specificity, and sensitivity measures for each subject and task. The behavioral data collected during the MEG recordings were used as the fMRI data were collected immediately after the MEG recordings, leading to potential learning effects influencing the task performance during fMRI data collection.

### MEG, fMRI, and PET data collection

All data (MEG, PET, and MRI) were collected from the same participants at the CERMEP imaging center (Lyon, France). The

Downloaded from https://academic.oup.com/cercor/advance-article/doi/10.1093/cercor/bhad522/7512628 by Jyvaskyla University user on 17 January 2024

MEG data were recorded in a magnetically shielded room using a 275-channel CTF whole-head system. The signals were band-pass filtered at 0.016–150 Hz and sampled at 600 Hz. The anatomical and functional magnetic resonance images were collected with a 1.5 Tesla scanner (Siemens Sonata Maestro Class). The T1-weighted anatomical MRIs were obtained with $1.0 \times 1.0 \times 1.0$ mm$^3$ resolution. The functional MRIs were acquired in three runs using a pulse sequence with repetition time/echo time (TR/TE) 2500/60 msec, flip angle = 90°, field of view (FOV; in-plane) = 220 mm, in-plane resolution 3.4 mm × 3.4 and slice thickness 4 mm, spacing between slices 4.4 mm. The PET data were recorded with a Siemens HR+ camera, and [11C]flumazenil (FMZ), an agent that binds to benzodiazepine (BZD) receptor, was used. FMZ (RO15-1788) was labeled with 11C, using the methylation process (Maziere et al. 1984). A dynamic 3D acquisition was applied providing 12 consecutive frames of 63 contiguous 2.42 mm thick slices, with an isotropic spatial resolution near 5 mm3 FWHM (full width at half-maximum). A 68Ge transmission scan was used to measure the attenuation correction. A partial saturation protocol consisting of a single intravenous injection of a mixture of 5 mCi of [11C]FMZ and 0.01 mg/kg of unlabeled FMZ was used, followed by acquisition of the emission data for 55 min. This single injection allowed the calculation of B'max parametric images, i.e. estimates of receptor density, without arterial blood sampling (Delforge et al. 1995).

## MEG data analysis

Neural activity estimates were obtained from the MEG signals with event-related Dynamic Imaging of Coherent Sources (erDICS), a beamforming technique in the time-frequency domain (Gross et al. 2001; Laaksonen et al. 2008). In erDICS, the cortical-level beamforming estimates are based on the sensor-level time-dependent cross-spectral density matrix (CSD), computed using Morlet wavelets. Here, wavelets with the width 7 cycles for every frequency were used to calculate the CSDs between 36 and 104 at 2 Hz resolution in the range from 500 ms before stimulus onset to 1500 ms post stimulus at 17 ms intervals. The width parameter defines both the spectral bandwidth and duration of the wavelets, with lower frequencies analyzed with longer wavelets that lead to lower temporal resolution, but higher frequency resolution compared with higher frequencies when a constant number of cycles is used across all frequencies (Cohen 2019). Trials in which the amplitude of either the vertical or the horizontal electro-oculogram exceeded 150 $\mu$V were rejected. In addition, the MEG data were examined visually and data segments that contained artifacts were excluded from the analysis. The beamforming estimates of cortical oscillatory power levels at different frequencies were computed, using a spherical head model, in a spatially equivalent grid across subjects. The grid, consisting of 3922 points, was constructed by creating a regular grid at 6-mm intervals in an atlas brain and by transforming this grid to the individual brains using Fieldtrip and SPM8 (Oostenveld et al. 2011). For the visualization of the data, the volumetric beamforming maps were project to the surface of the brain with Freesurfer (Fischl 2012).

## fMRI data analysis

The fMRIs data analysis was conducted with SPM8 (Wellcome Department of Imaging Neuroscience, London, United Kingdom). The first four volumes were discarded to allow for magnetic saturation effect. The functional images were slice-time corrected, realigned to the first image of the first run and then co-registered with the anatomical MRI. The realigned and co-registered images were then normalized to the standard SPM8 echo-planar image template and smoothed with an 8-mm FWHM isotropic Gaussian kernel. The data were high-pass filtered with a cut-off frequency of 1/510 Hz and serial correlations were compensated for by using a first order autoregressive model. The preprocessed data were included in a general linear model (GLM) that included the three WM condition (1-, 2-, and 3-back) and rest as well as movement parameters as nuisance regressors. The individual-level fMRI data were spatially normalized to the MNI template in SPM8 for group-level estimation of the WM-load dependent modulations.

## PET data analysis

Static PET images were obtained by summing frames 8–12 from the dynamic imaging (corresponding to the acquisition period from 20 to 55 min post-injection). These static images of the PET volumes were realigned to the anatomical MRIs. Ten-millimeter circular ROIs were placed over the midportion of the pons, a suitable reference region for the calculation of the nonspecific FMZ binding60; the reference encompassed 7–9 consecutive MRI slices displaying that structure. These ROIs were then transferred onto the corresponding FMZ-PET slices. An additional circular ROI with 15 mm diameter was placed over the occipital cortex which commonly displays a high concentration of BZD receptors (Innis et al. 1991). A partial-saturation model, based on a Scatchard plot, was then used to obtain the B'max parametric images (Delforge et al. 1997). In this model, the free ligand concentration is estimated in the pons, whereas the range of the bound ligand concentration is evaluated in the occipital cortex. Using this approach we obtained, for each subject, a set of 63 contiguous 2.42 mm thick parametric images of BZD receptor B'max. Each individual's PET data were smoothed using a $15 \times 15 \times 21$ mm FWHM Gaussian kernel; the level of smoothing was chosen to achieve similar resolution to the MEG estimates of neural activity (Gross et al. 2003). The PET-data were co-registered with each individual's anatomical MRI in SPM8.

## ROI identification

ROIs were identified separately based on the MEG and fMRI data. For MEG, estimates of oscillatory power were computed in three distinct time windows (0–500, 500–1000, and 1000–1500 ms post stimulus) in each of the three WM tasks. These individual-level power maps were normalized by dividing them by the standard deviation of mean baseline activity (−500 to 0 ms) across the three WM tasks across all grid points. The ROIs within each time window were obtained by contrasting the average oscillatory activity of the 3- and 2-back tasks with the activity of the 1-back task and by identifying clusters that showed significant activity at the group level (Wilcoxon signed rank test, $P < 0.05$, cluster-size > 50, $n = 10$). Here, it would have also been possible to use ROIs known to be involved in WM or to use repeated measures tests to evaluate systematic magnitudes/rankings across the three WM-conditions. However, as we wanted to identify regions showing WM-related modulations specifically for the present cohort as well as to utilize the same data for the ROI identification and correlations analyses (see section "Correlation analyses in the ROIs" below), the present bi-variate approach was used. The fMRI ROIs were identified in a similar manner. First the beta-parameters for all WM tasks in each individual were normalized by dividing them with the standard deviation of the beta-parameters during rest in the whole brain. The average of the beta-parameters of 3- and 2-back tasks were then contrasted to the beta-values during the 1-back task and clusters that showed significant activity at the group level were identified (Wilcoxon signed rank test, $P < 0.05$, cluster-size > 300, $n = 10$).

Downloaded from https://academic.oup.com/cercor/advance-article/doi/10.1093/cercor/bhad522/7512628 by Jyvaskyla University user on 17 January 2024

## Correlation analyses in the ROIs

Within the identified ROIs, we estimated correlations between both the neural (MEG, fMRI, PET) and behavioral measures. For the MEG data, we determined in each ROI the individual-level peak amplitude and frequency within the range between 40 and 100 Hz. Here, the data were averaged across all grid points within the ROI. In this analysis, we averaged the data across an 8 Hz window at each bin to reduce the effects of noise (e.g. estimate of activity of 40 Hz was calculated based on the average CSD at the interval of 36–44 Hz). The peak frequencies were computed by identifying the frequency for which the ratio of activity between the average of 3- and 2-back tasks and the 1-back task was maximal. The amplitude modulation for each subject was obtained by subtracting the activity during the 1-back task from the average activity during the 3- and 2-back tasks at this frequency. In this analysis, each subject's data were normalized by the standard deviation in all grid points across all frequency bins in the baseline time-window (−500–0 ms with respect to stimulus presentation across the three n-back tasks). The standard deviation-based normalization was chosen as in n-back tasks the baseline time-window comprises also WM-specific neural activity and by subtracting this activity from the post-stimulus data does not necessarily lead to the accurate quantification of amplitude modulations. The chosen approach, computed across all source locations and frequencies only some of which represent tasks-relevant signals should, in turn, yields a good estimate of random fluctuations within the data whose magnitude depends on the subject-specific overall strength of the MEG recordings. Accordingly, the approach yields normalized estimates that allow comparing the values across subjects (Dale et al. 2000). Parametric modeling of the spectra within individual conditions with FOOOF (Donoghue et al. 2020) did not systematically detect gamma-band oscillatory peaks in all subjects in every identified cluster. In the fMRI data, we first averaged the beta-values across the voxels within the ROI. These beta-parameters were normalized by dividing them with the standard deviation of the beta-parameters during rest in the whole brain. The individual-level modulation of BOLD activity within each ROI was then determined by subtracting the activity during the 1-back task from the average activity during the 3- and 2-back tasks. For the PET data, we determined for each MR-voxel within the MEG and fMRI ROIs the closest corresponding PET voxel and defined the unique set of these PET voxels for each ROI. As the measure of $GABA_A$ receptor density in each ROI, we used the average of $GABA_A$ receptor density in these PET voxels. The correlations between the different neural measures and between neural and behavioral measures were computed using Spearman's rho ($n = 10$). As with low number of subjects the correlation estimates may be influenced by outliers in the data, we computed the 95% confidence limits for the correlation estimates using bootstrapping for both the correlations across the neural data as well as between neural and MEG-based behavioral data ($n = 10$ in all bootstrapping analyses). In the approach we left out data pairs for 2 random subjects 200 times and computed the correlation values for the re-sampled data. From the obtained distribution of 200 correlation values, we calculated the 95% upper and lower confidence limits. This procedure was applied to all correlation analyses showing significant findings with the full sample of subjects. To evaluate the predictive value of the observed correlation patterns, we also used a leave-two-out-based classification analysis to test whether the linear relationship between data types (e.g. $GABA_A$ receptor density and gamma peak frequency) observed within a sub-sample of eight subjects would correctly predict the relationship for the left-out subjects. Here, a polynomial of degree one was used as the linear model. The eight subjects for the training data were randomly drawn 500 times and for each round we labeled for the predicted data type (e.g. predicted gamma frequency based on the subject's $GABA_A$ receptor density) the subject whose true value was closer to the predicted one. This procedure yielded 1000 incorrect/correct classifications, allowing to determine the overall classification accuracy. The 99% confidence limit for the classification was obtained by randomly conducting the same procedure 200 times with random pairings of the two data types for the eight subjects whose data were used in the training. We also examined using multiple linear stepwise backward regression in SPSS 28.0 (IBM) the possible joint effect of the imaging measures on the behavioral data. The analyses were conducted separately for MEG- and fMRI-specific ROIs, i.e. MEG-measures were examined jointly with $GABA_A$ receptor density only in the ROIs identified based on MEG modulations. In the analysis, we applied the default parameters (e.g. $P \geq 0.1$ removal criterion) within the stepwise backward regression. Unless mentioned otherwise, for all correlations and regression analyses reported here we used uncorrected $P$-values.

# Results

To investigate the interplay between high-frequency neural oscillations, hemodynamics and GABAergic inhibition, we measured gamma-band oscillations with MEG, BOLD activity with fMRI, and $GABA_A$ receptor density using FMZ-PET all in the same population of healthy individuals. The characteristics of oscillatory neuromagnetic signals and BOLD dynamics in each individual were assessed during the performance of a standard n-back visual WM task. The FMZ-PET data used to determine the $GABA_A$ receptor density were collected while the subjects were resting in the scanner. Individual subject WM performance was probed using multiple behavioral metrics (reaction times, accuracy, sensitivity, and specificity) based on the subjects' responses during the MEG experiment. We leveraged this combination of data to probe the relations between behavior and the different neural measures specifically in brain regions showing load-dependent modulation of activity during WM (see Fig. 1).

## ROI identification based on the modulation of gamma-band and BOLD activity

For both the MEG and fMRI data, the average activity during the high memory-load conditions (3- and 2-back) was contrasted to the activity during the 1-back task ($P < 0.05$, see Fig. 2), where the MEG investigation was done in three distinct time windows following each stimulus (0–500, 500–1000, and 1000–1500 ms). ROIs (2 in MEG, 5 in fMRI; see Table 1, Figs 4 and 5) were identified from these voxel-level maps by determining contiguous clusters per modality and time window. The ROI labels in Table 1 do not represent any specific parcellation schemes but, instead, give approximate information on the main cortical regions the observed effects extend to. Note also that the extents of the ROIs do not necessarily accurately represent the true extents of the relevant modulations as the observed effects depend on the selected source-modeling approach and the chosen statistical threshold.

## The relationship between $GABA_A$ receptor density, gamma-band power, and BOLD activity

In the clusters identified based on gamma-band power modulations, peak modulation frequency was identified by comparing the average activity between the 3- and 2-back conditions to

Downloaded from https://academic.oup.com/cercor/advance-article/doi/10.1093/cercor/bhad522/7512628 by Jyvaskyla University user on 17 January 2024

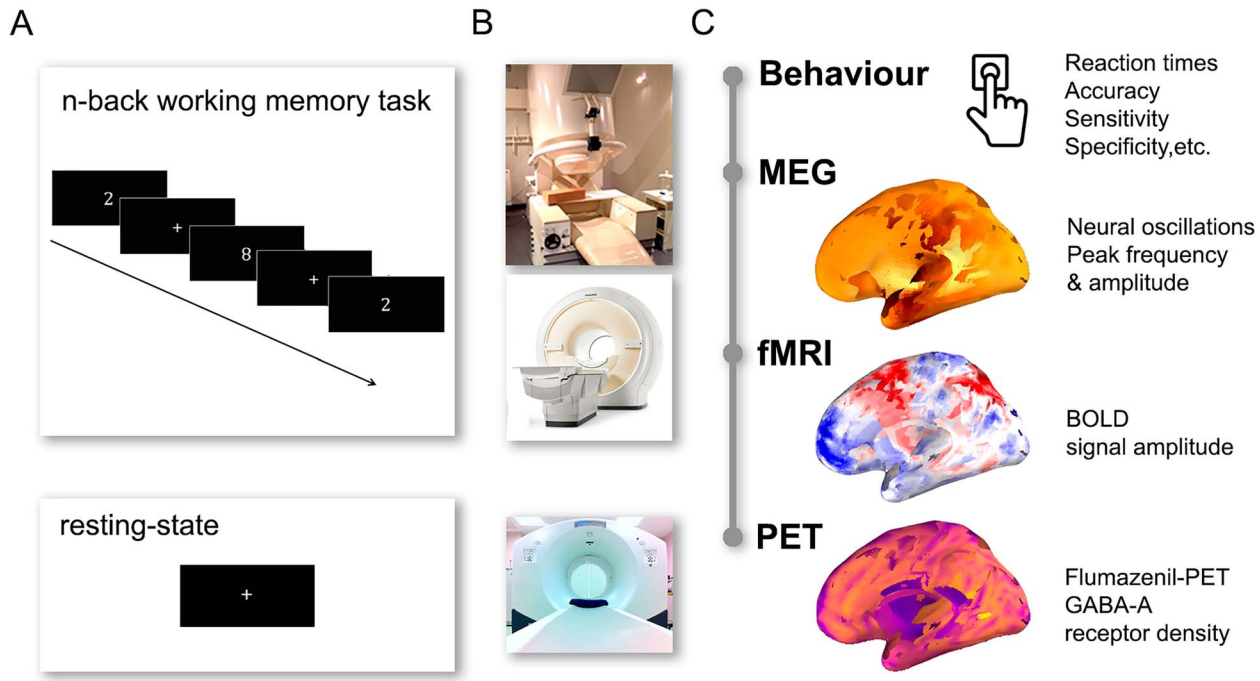


**Fig. 1.** The study consisted of the collection of multimodal neuroimaging data during an n-back task and the determination of the relationship between the neuroimaging signals and their link to WM task performance. (A) MEG and fMRI data were collected during the experimental task which consisted of 1-, 2-, and 3-back tasks of visually presented letters, while FMZ-PET data were collected during rest. (B) From the experimental data, we determined (C) the WM task performance measures (reaction times, accuracy, sensitivity, and specificity) as well as measures of oscillatory (peak frequency and amplitude) and hemodynamic (BOLD signal amplitude) activity, whereas the FMZ-PET data collected during rest were used to determine $GABA_A$-receptor densities across the brain.

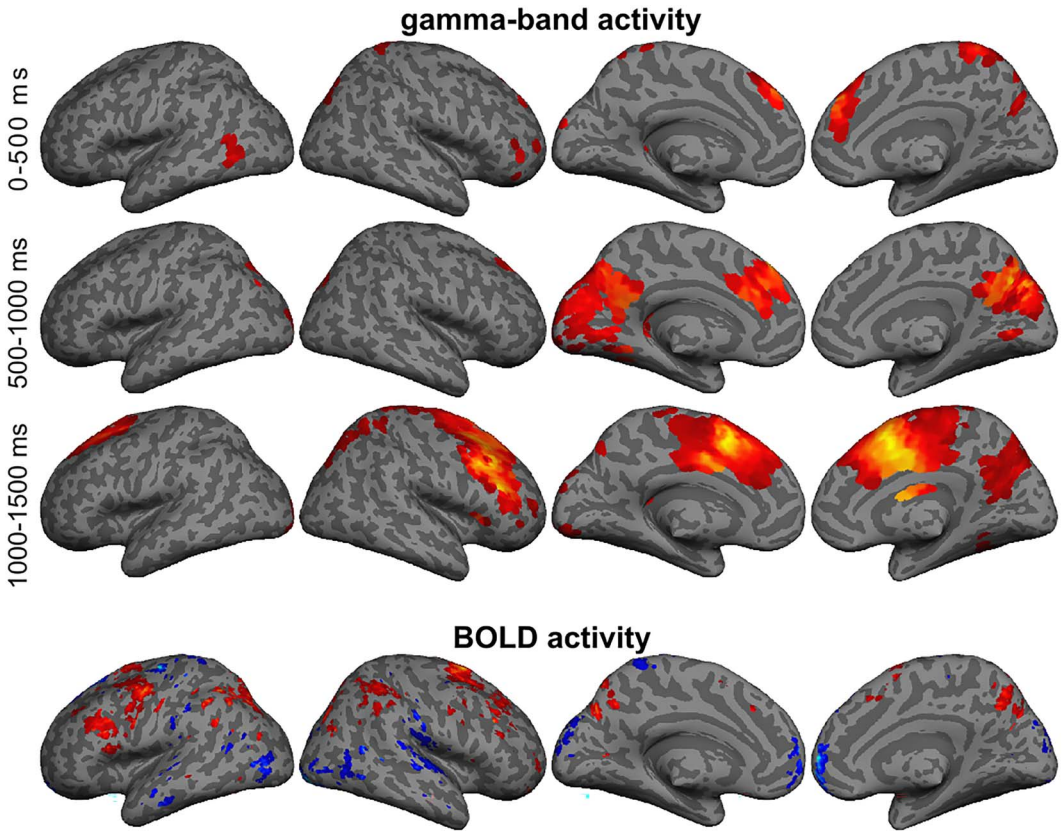


**Fig. 2.** Brain areas showing significant modulation of activity as a function of memory load for MEG and fMRI ($P < 0.05$). Areas showing more neural/hemodynamic activity during conditions with a higher memory load are shown in red/yellow and areas showing less activity in blue. For visualization purposes, the volumetric data are projected to the surface of the brain.

Downloaded from https://academic.oup.com/cercor/advance-article/doi/10.1093/cercor/bhad522/7512628 by Jyvaskyla University user on 17 January 2024

**Table 1.** ROIs identified based on MEG and fMRI data (MEG1: 500–1000 ms; MEG2: 1000–1500 ms).

| ROI | ROI size | Brain region | Brodmann | L/R | x | y | z |
|---|---|---|---|---|---|---|---|
| MEG1 | 248 | Cuneus | 18 | L/R | −1 | −70 | 21 |
| MEG2 | 737 | Medial Frontal Gyrus | 6 | L/R | −1 | 15 | 44 |
| | | Middle Frontal Gyrus | 9 | R | 40 | 27 | 30 |
| fMRI1 | 1567 | Precentral Gyrus | 6 | L | −50 | −3 | 46 |
| | | Middle Frontal Gyrus | 46 | L | −41 | 18 | 22 |
| fMRI2 | 1157 | Precuneus | 7 | L/R | −10 | −65 | 46 |
| fMRI3 | 407 | Inferior Parietal Lobule | 40 | R | 43 | −38 | 41 |
| fMRI4 | 998 | Superior Frontal Gyrus | 6 | R | 21 | 12 | 59 |
| fMRI5 | 404 | Temporo-Parietal Junction | 13 | R | 40 | −25 | 11 |

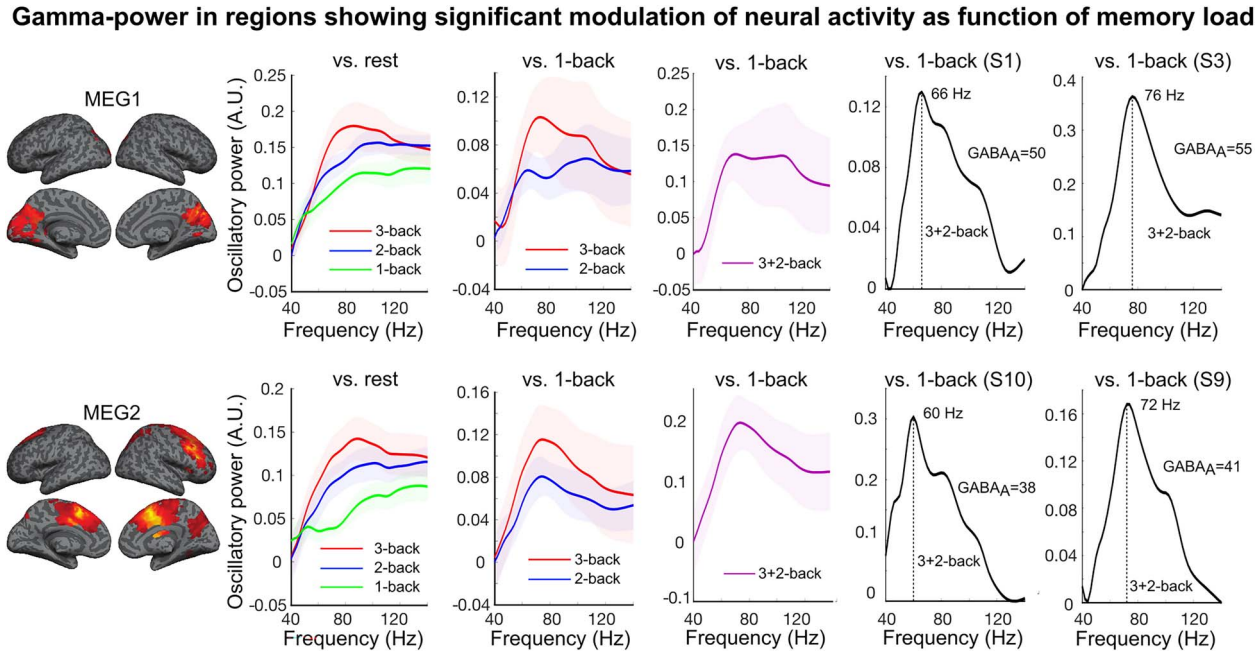


**Fig. 3.** Group- (first three panels) and individual-level (last two panels) gamma-band spectra in the two MEG clusters of interest for the different WM comparisons. In the group-level spectra, confidence intervals represent the grand average ± SEM values. The vertical dashed line in the individual-level spectra represents the identified peak modulation frequencies, shown next to the peaks. $GABA_A$-receptor densities in the graphs represent the average values within the MEG clusters for each of the example subjects.

the 1-back condition (see Fig. 3 and Supplementary Fig. 8). This approach to identifying peak gamma frequency (and gamma amplitude at this frequency) was used to examine the relationship between individual gamma-band profiles and GABAergic inhibition across participants. This approach is fine-tuned to detecting peaks in gamma oscillations that are specific to WM as they are derived from identifying load-related increases in broad-band high-frequency activity (Carver et al. 2019).

In both MEG ROIs (Cuneus and Medial/Middle Frontal Gyrus), we found a significant positive correlation (Spearman's rho, $P < 0.05$) between the $GABA_A$ receptor density and the peak frequency of the gamma-band activity. The 95% confidence intervals of the rho values were between 0.43 and 0.88 for the two ROIs (Cuneus, $CI_{95\%}$, 0.46–0.88; Medial/Middle Frontal Gyrus, $CI_{95\%}$, 0.43–0.83). In both, ROIs, the classification analysis suggested that the relationship determined based on a subsample of the subjects was predictive of the relationship in the other subjects (Cuneus: accuracy = 66.4%, $CL_{99\%}$ = 56.95%; Medial/Middle Frontal Gyrus: accuracy = 58%, $CL_{99\%}$ = 49.95%). In contrast, the correlation between receptor density and gamma amplitude did not reach significance (Fig. 4). As far as the fMRI ROIs are concerned, we found a significant negative correlation between BOLD amplitude and $GABA_A$ receptor density in the Precuneus ($CI_{95\%}$, −0.38 to 0.95). The classification analysis showed a significant predictive value for this relationship (accuracy = 63.5%, $CL_{99\%}$ = 55.6%). The correlations in the other four ROIs were not significant (Fig. 5). No significant correlations were detected between BOLD amplitude and gamma peak-frequency or amplitude (see Supplementary Fig. 1).

## Behavioral performance during the WM task

The performance of the subjects during the WM task was determined by quantifying the reaction times for each of the tasks (1-, 2-, and 3-back) and the number of incorrect and correct responses, and by deriving the accuracy, sensitivity, and specificity scores based on the number of responses. These measures (see Table 2) show the expected decrease in performance as a function of memory load and a marked increase in reaction times in the 2- and 3-back conditions compared with the 1-back task (reaction times for correct responses in 3- and 2-back vs. 1-back condition, Wilcoxon signed rank test, $P < 0.01$). The other behavioral measures showed similar effects, with significant differences between

Downloaded from https://academic.oup.com/cercor/advance-article/doi/10.1093/cercor/bhad522/7512628 by Jyvaskyla University user on 17 January 2024

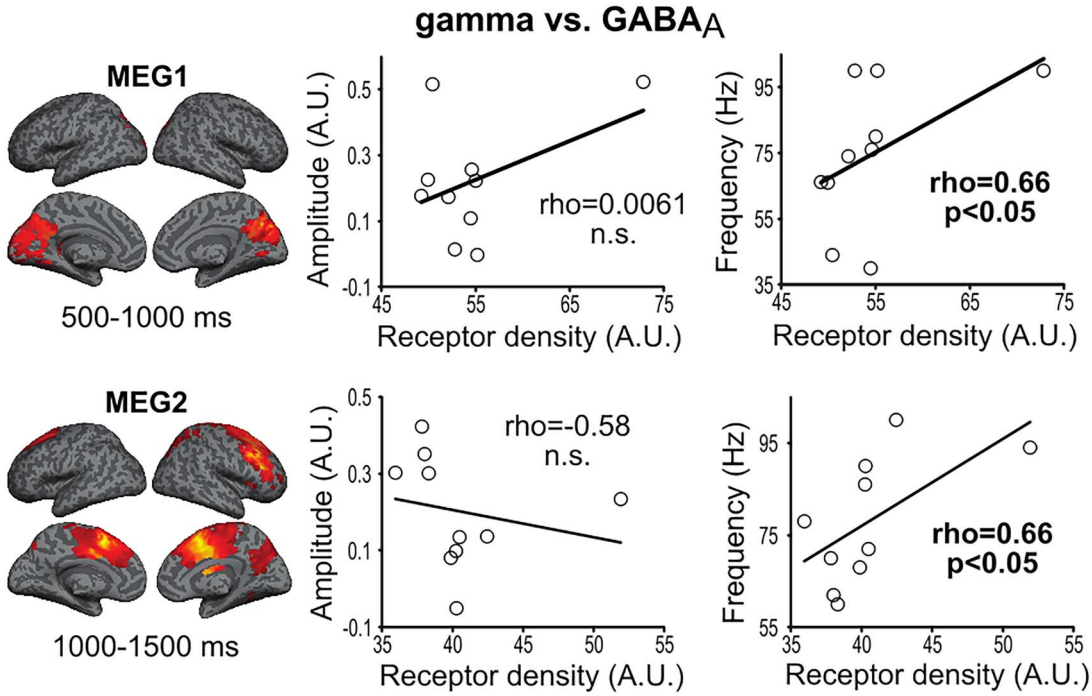


**Fig. 4.** Correlation (Spearman's rho) between $GABA_A$-receptor density and gamma-band peak amplitude and frequency in brain areas showing significant modulation of activity as a function of memory load. The x-axis portrays the mean receptor density (A.U.). The correlations were examined in two ROIs (MEG1: Cuneus; MEG2: Medial/Middle Frontal Gyrus). See Table 1 for the sizes, Brodmann areas, and Talairach coordinates of the ROIs.

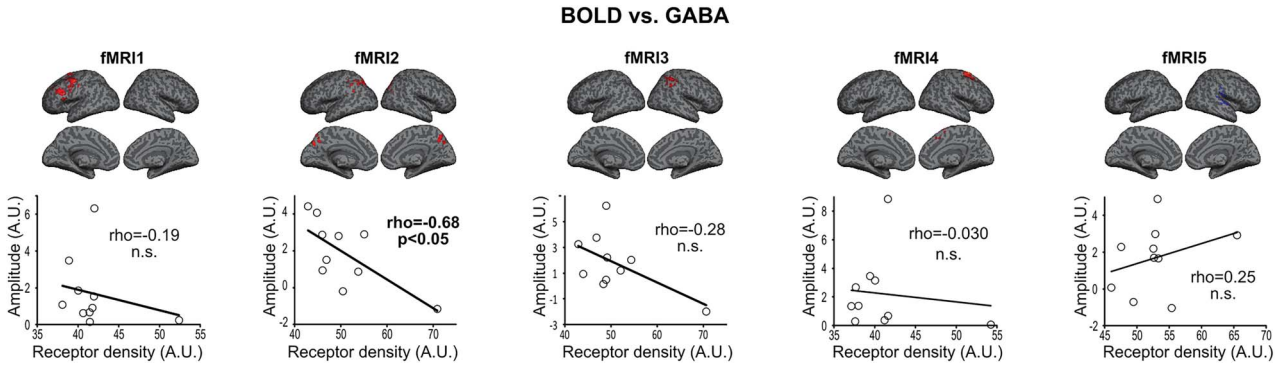


**Fig. 5.** Correlation (Spearman's rho) between $GABA_A$-receptor density and BOLD amplitude in brain areas showing significant modulation of activity as a function of memory load. The x-axis portrays the mean receptor density (A.U.). The correlations were examined in five ROIs (fMRI1: precentral/middle frontal gyrus; fMRI2: precuneus; fMRI3: inferior parieral lobule; fMRI4: superior frontal gyrus; fMRI5: temporo-parietal junction). See Table 1 for the sizes, Brodmann areas, and Talairach coordinates of the ROIs.

3- and 1-back conditions for accuracy, sensitivity, and specificity ($P < 0.01$) and between 2- and 1-back conditions for sensitivity and accuracy ($P < 0.05$; specificity, $P = 0.31$).

## The relationship between $GABA_A$ receptor density and WM reaction times

When we computed correlations between the neural measures (gamma-band and BOLD activity, $GABA_A$ receptor density) and the different behavioral measures (reaction times, accuracy, sensitivity, specificity), we found significant correlations (Spearman's rho) only between the $GABA_A$ receptor density and reaction times measures (see Supplementary Table 1). In the 2 MEG and 5 fMRI ROIs, the $GABA_A$ receptor density showed significant negative correlation with reaction times in the 3-back task in the Inferior Parietal Lobule ($CI_{95\%}$, −0.60 to −0.88) and Temporo-Parietal Junction ($CI_{95\%}$, −0.62 to −0.93; see Fig. 6). In both regions, the classification analysis suggested that the relationship determined in a set of subjects would correctly predict the relationship between $GABA_A$ receptor density and reaction times in other subjects (Inferior Parietal Lobule: accuracy = 65.7%, $CL_{99\%}$ = 50.45%; Temporo-Parietal Junction: accuracy = 65.5%, $CL_{99\%}$ = 51.7%). Across the ROIs, the $GABA_A$ receptor density showed significant negative correlation with the reaction times difference between the 3- and 1-back tasks in the Medial/Middle Frontal Gyrus ($CI_{95\%}$, −0.50 to −0.79), Inferior Parietal Lobule ($CI_{95\%}$, −0.60 to −0.79) and Temporo-Parietal Junction ($CI_{95\%}$, −0.50 to −0.81). In all these regions, the classification analysis yielded significant results in predicting the reaction times difference from the $GABA_A$ receptor density (Medial/Middle Frontal Gyrus: accuracy = 67.6%, $CL_{99\%}$ = 53.8%; Inferior Parietal Lobule: accuracy = 69.8%, $CL_{99\%}$ = 54.55%; Temporo-Parietal Junction = 68.3%, $CL_{99\%}$ = 54.05%). We also tested whether the reaction times were associated with the $GABA_A$ receptor density in cortical motor regions. The correlation between the reaction times measures and

Downloaded from https://academic.oup.com/cercor/advance-article/doi/10.1093/cercor/bhad522/7512628 by Jyvaskyla University user on 17 January 2024

**Table 2.** Behavioral performance in the WM tasks.

| Behavioral measure | 1-back | 2-back | 3-back |
|---|---|---|---|
| Correct responses | 113.8 | 114.5 | 92.3 |
| Incorrect responses | 1.6 | 3.6 | 16.5 |
| Accuracy | 0.986 | 0.969 | 0.847 |
| Sensitivity | 0.964 | 0.926 | 0.717 |
| Specificity | 0.998 | 0.990 | 0.899 |
| Reaction times (ms) (correct responses) | 356.4 | 445.6 | 486.7 |
| Reaction times (ms) (incorrect responses) | 388.7 | 527.5 | 599.2 |

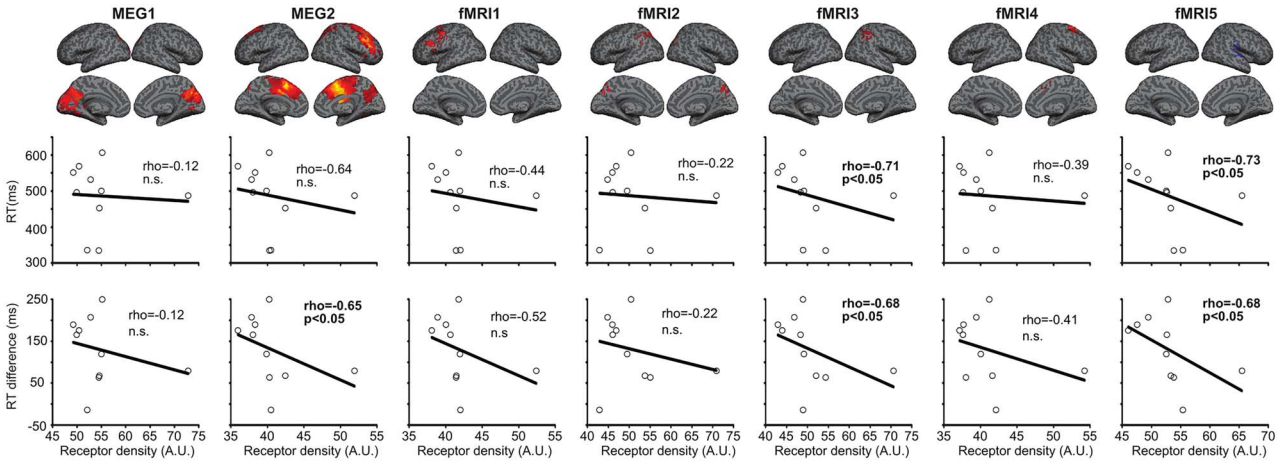


**Fig. 6.** Correlation (Spearman's rho) between $GABA_A$-receptor density and reaction times during the WM tasks in the ROIs identified based modulation of activity as a function of memory load. The tested reaction-time measures represent the correct responses in the 3-back task (RT) and the difference between the correct responses in 3- and 1-back tasks (RT difference). See Table 1 for the anatomical descriptions, sizes, Brodmann areas, and Talairach coordinates of the ROIs. For visualization purposes, the volumetric data are projected to the surface of the brain.

$GABA_A$ receptor density in the anatomically defined Precentral Gyrus (Desikan et al. 2006) were not significant neither in the left ($GABA_A$ vs. reaction times in the 3-back task: rho = −0.41, $P = 0.25$; $GABA_A$ vs. reaction times difference between the 3- and 1-back tasks: rho = −0.44, $P = 0.20$) nor the right hemisphere ($GABA_A$ vs. reaction times in the 3-back task: rho = −0.58, $P = 0.088$; $GABA_A$ vs. reaction times difference between the 3- and 1-back tasks: rho = −0.55, $P = 0.10$). The whole brain analysis of the relationship between reaction times and $GABA_A$-receptor density did reveal smaller significant clusters within the precentral gyrus, but these did not survive correction for multiple comparisons (see Supplementary Fig. 7).

## Results in other frequency bands

We also tested whether the amplitude or frequency properties of oscillations in other bands (theta, alpha, beta) would show any correlations with the receptor density in regions that exhibit memory load-dependent activity within these frequency bands (see Supplementary Fig. 2 and Supplementary Table 2). Across the ROIs identified in the theta, alpha, and beta bands, no significant correlations were detected between neural activity and $GABA_A$ receptor density (see Supplementary Fig. 3).

## Extension to more general task-based modulations (WM TASK vs. REST)

The primary focus in this study has been on brain regions that exhibit memory load-dependent brain activity modulations, i.e. areas identified by comparing the activity between the 3- and 2-back conditions to the 1-back condition. However, for completeness, we also contrasted the WM task condition to resting data in order to identify regions more generally involved in the WM task (see Supplementary Fig. 4 and Supplementary Table 3). These TASK vs. REST analyses revealed that in the Middle Occipital Gyrus, $GABA_A$-receptor density correlated positively with the gamma-band peak frequency and negatively with the BOLD amplitude (see Supplementary Fig. 5), which is in line with and confirms observations reported in previous studies (Muthukumaraswamy et al. 2009; Kujala et al. 2015). This analysis also revealed a positive correlation between the BOLD amplitude and $GABA_A$-receptor density in the left Inferior Parietal Lobule. In several of the ROIs identified based on the modulation of gamma-band or BOLD activity (Postcentral Gyrus, Inferior Parietal Lobule, Middle Occipital Gyrus), significant correlations (see Supplementary Table 4 and Supplementary Fig. 6) were detected between the $GABA_A$-receptor density and reaction times as well as between the BOLD amplitude and reaction times in one ROI (Middle Occipital Gyrus).

## Joint influence of imaging measures on behavior

We also examined using multiple linear stepwise backward regression whether the different imaging measures would jointly explain the variability in the behavioral measures across the ROIs identified based on the WM-load dependent as well as TASK vs. REST modulations. The analysis revealed that for isolated ROI and behavioral measure combinations the behavioral variability could be better explained by two vs. one imaging measure (see Supplementary Data for full list of significant/marginally

Downloaded from https://academic.oup.com/cercor/advance-article/doi/10.1093/cercor/bhad522/7512628 by Jyvaskyla University user on 17 January 2024

significant findings). Such findings were made for the combination of $GABA_A$ receptor density estimates with both MEG and fMRI amplitude, and for several behavioral measures (reaction times difference, accuracy, sensitivity). This was particularly the case for cluster in the Postcentral gyrus (identified in MEG TASK vs. REST contrast), in which the best linear model for explaining both accuracy and sensitivity consisted of the $GABA_A$ receptor density and MEG amplitude modulation.

## Discussion

We combined fMRI, MEG, and FMZ-PET-based estimates of $GABA_A$ receptor density within the same subject cohort to probe the relationships between GABAergic inhibition, hemodynamic modulations and oscillatory activity, in an attempt to achieve a more holistic view of the neural mechanisms underlying WM. Our primary goal was to elucidate the relationship between the neural activity, hemodynamics and neurotransmitter measures in higher-order regions, a question that has previously been addressed in humans primarily only in sensory and motor regions. In contrast to previous work, we focused specifically on regions showing modulation of activity as a function of WM load and found that $GABA_A$-receptor density correlated positively with the peak frequency of gamma-band power modulations and negatively with BOLD amplitude in such areas. Interestingly, when we compared the different neural measures to behavioral parameters, we found significant correlations exclusively between the $GABA_A$ receptor density and WM reaction times in the Inferior Parietal Lobule, Temporo-Parietal Junction and Medial/Middle Frontal Gyrus. These observations align well with our hypotheses building on previous studies examining the relationship between gamma-band activity and GABA in primary sensory cortices (Muthukumaraswamy et al. 2009; Kujala et al. 2015), GABA and BOLD dynamics (Northoff et al. 2007), and the importance of the GABAergic system of explaining the individual task-performance (Edden et al. 2009). Our findings demonstrate that GABAergic inhibition is central in shaping gamma oscillations and hemodynamic activity in higher-order regions and in explaining the between-subject performance variability on the WM task.

Contrasting high vs. low memory load conditions revealed modulation of gamma-band activity in the bilateral Cuneus and Medial/Middle Frontal Gyrus. In both regions, the gamma peak modulation frequency (but not amplitude) correlated with the $GABA_A$ receptor density measured in the same areas at rest. Significant correlation between the $GABA_A$ receptor density and gamma peak frequency was detected also in the Poscentral Gyrus, which showed modulation of activity in TASK vs. REST. These findings extend previous neuroimaging results in the primary visual cortex (Muthukumaraswamy et al. 2009; Kujala et al. 2015) as well as from animal and modeling studies supporting the role GABAergic inhibitory interneurons in the generation and shaping of gamma-band oscillations (Brunel and Wang 2003; Whittington and Traub 2003; Bartos et al. 2007). Importantly, our findings indicate that the mechanisms of gamma-band oscillations follow the same principles in higher-order human cortical regions as seen in the primary sensory regions as well in animal models. Notably, for the present data, the gamma-band peak frequency was best identified via the ratio of neural activity between high and low WM load conditions (see Fig. 3 and Supplementary Fig. 8). These spectra revealed also potentially interesting differences across subjects, with single and multiple peaks within the gamma bands as well as differences in the presence of sustained high-frequency (>100 Hz) activity. Accordingly, the gamma-band modulation spectra show effects other than the main peak frequency whose relationship with the GABAergic system was not explored within the present study. Interestingly, the original findings demonstrating link between the GABAergic system and gamma oscillations in humans using MRS-based estimates of GABA concentration (Muthukumaraswamy et al. 2009) were not replicated when the same phenomena were studied in a larger cohort (Cousijn et al. 2014). Here, as in our previous study (Kujala et al. 2015), we used PET-FMZ based estimates of $GABA_A$ receptor density and detected correlations between the gamma-band peak modulation frequency and receptor density in both higher- and lower-order brain regions. This suggests that the PET-FMZ based estimation of GABAergic system may provide a better proxy than the MRS based estimates which do not dissociate the contributions of the neurotransmitter metabolic pool from the synaptic pool (Stokes et al. 2014). This notion aligns with the high test–retest reliability of PET-FMZ based measurements (Salmi et al. 2008). The present finding should, however, be replicated in a larger cohort to corroborate the value of PET-FMZ based quantification of the GABAergic system for evaluating the generation of gamma-band oscillations. It should also be noted that the synaptic specificity of FMZ is limited as it binds also to extrasynaptic subunits of GABA-BZD receptors. Specific synaptic properties could potentially be better captured by using the inverse agonist GABA-BZD receptor PET tracer [11C]Ro15-4513 (Myers et al. 2012). Here, we interpreted according to the common view that the PET-based estimates that depend on the binding of FMZ to the $\alpha$-subtype of $GABA_A$ receptors to represent $GABA_A$ receptor density. While these estimates can be influenced by, e.g. extrasynaptic binding, animal studies suggest that the FMZ-based estimates measure accurately the occupancy of the $\alpha$-subtype of $GABA_A$ receptors (Müller Herde et al. 2017). Moreover, within the present cohort of healthy subjects there should not be subject-specific losses of pyramidal neurons that may also underlie differences in $GABA_A$ receptor density estimates across subject populations (Lloyd et al. 2000). Thus, while the receptor density estimates could be improved by using, e.g. [11C]Ro15-4513, the PET-FMZ based measure used in the present study should represent specifically $GABA_A$ receptor density as opposed to other neuronal properties. However, the present data do not allow us to identify possible reasons for the observed variability in the receptor density across subjects. It should also be noted that in the present study the focus was on examining the relationships between different neural measures in ROIs that average the $GABA_A$ receptor density estimates across extended sets of voxels. Accordingly, the analyses are insensitive to local variations in different neural properties such as synaptic and extrasynaptic binding. For spatially more detailed examinations the specificity of the PET binding agent might play a larger role. Moreover, in such investigations, it could be beneficial to maximize the resolutions of the MEG and fMRI estimates by, e.g. using realistic conductor models in MEG and higher field strengths in fMRI.

Previous studies have shown that BOLD amplitude correlates negatively with GABA concentration in several cortical regions (Northoff et al. 2007; Muthukumaraswamy et al. 2009; Jung et al. 2017). Here, we detected the same phenomenon in the higher-order regions showing modulation of BOLD activity as a function of memory load (left Parietal Cortex and bilateral Precuneus) as well in the Middle Occipital Gyrus that showed modulation of activity in TASK vs. REST. This demonstrates that the PET-FMZ-based measure of $GABA_A$ receptor density facilitates the study of the relationship between the GABAergic system and hemodynamics, allowing such investigations to be conducted with improved

Downloaded from https://academic.oup.com/cercor/advance-article/doi/10.1093/cercor/bhad522/7512628 by Jyvaskyla University user on 17 January 2024

spatial resolution compared with MRS-based studies. However, the observed relationship between BOLD and $GABA_A$ receptor density was not as robust as for the MEG ROIs, as significant correlations were detected in three of the four MEG ROIs but only in three of the eleven fMRI ROIs. This suggests either that PET-FMZ-based estimates do not sufficiently capture the GABAergic underpinnings of BOLD dynamics, or that due to the specific properties and complexity of the BOLD response (Logothetis 2008; Bandettini 2012), the relationship between $GABA_A$ receptor density and BOLD response is not as straightforward as between gamma-band oscillations and receptor density. Furthermore, it is possible that the use of 1.5 T scanner compared with scanners with higher field strengths may have reduced the sensitivity of the fMRI analyses, leading to underrepresentation of the link between BOLD dynamics and the GABAergic system in the present study.

In neuroimaging studies, the GABAergic system has been linked previously to various behavioral measures such as orientation discrimination, perceptual acuity and dynamics, time perception and subconscious motor processing (Edden et al. 2009; Boy et al. 2010; Yoon et al. 2010; van Loon et al. 2013; Terhune et al. 2014; Kolasinski et al. 2017). Notably, it has been shown that in visual competition, the concentration of GABA in the frontal eye field correlated negatively with the subject's motor decision speed (Sumner et al. 2010). This observation aligns with our findings that $GABA_A$ receptor density in several higher-order regions (Inferior Parietal Lobule, Temporo-Parietal Junction and Medial/Middle Frontal Gyrus) correlated negatively with reaction times in the WM task. However, in contrast to the study by Sumner et al. (Sumner et al. 2010), the speed of WM task performance in our study correlated with properties of the GABAergic system in higher-order regions that do not directly control muscle movements. This finding suggests that GABAergic properties of regions responsible for the storage and manipulation of items in WM also affects the speed of processing in n-back tasks, likely via facilitation of the related decision making. This notion is further supported by our observation of a negative correlation between $GABA_A$ receptor density and reaction times in regions showing modulation of activity for TASK vs. REST. Here, significant correlations were detected in the Postcentral Gyrus, Middle Occipital Gyrus and Inferior Parietal Lobule—regions that do not directly control the motor output either. In our study, we did not observe significant correlation between $GABA_A$ receptor density in the precentral gyrus and reaction-time measures, indicating that performance in the WM task (as measured by the reaction times) is more driven by properties of higher-order brain areas supporting WM than by regions directly controlling the motor output. Nor did we detect any significant correlations between $GABA_A$ receptor density and other behavioral measures (accuracy, specificity, sensitivity). One possible explanation for this is that the other behavioral scores show markedly less variability across subjects than reaction time measures, and that to capture these effects, a larger cohort of subjects would have been required. Along the same lines, no significant correlations were detected between the other behavioral measures and modulations of gamma-band and BOLD activity in higher-order cortical regions. However, while we did not detect significant correlations between MEG and behavioral measures, in two of the four MEG ROIs (Cuneus, Postcentral Gyrus), the correlations between gamma-band amplitude and accuracy, sensitivity and specificity scores were predominantly negative, aligning with previous findings (Honkanen et al. 2015). We also applied multiple stepwise backward linear regression to test whether the imaging measures would jointly explain the behavioral variability in task performance. Such effects were detected particularly for the MEG ROIs identified via the TASK vs. REST contrast, for which the reaction times difference was best explained by the joint information in gamma-amplitude and $GABA_A$ receptor density in both the Middle Occipital Gyrus and right Parietal lobule and where the task accuracy was best explained by the joint information in gamma-amplitude and $GABA_A$ receptor density in the right Parietal Lobule. These finding pose the interesting notion that the static properties of the GABAergic system (here $GABA_A$ receptor density) and task-specific neural modulations would jointly predict how well an individual performs in WM tasks. However, considering the small number of these findings across the conducted tests, their moderate statistical significance and the small sample size of the study, this interpretation should be taken with caution.

The different neural signaling measures (oscillations, hemodynamics, GABA) we examined have all been studied extensively within the field of WM and memory function. For these measures, we detected significant correlations with behavior almost exclusively for $GABA_A$ receptor density, demonstrating the importance of the GABAergic system in WM and memory function. Work on freely moving and behaving mice and rats has demonstrated that cholecystokinin-expressing GABAergic neurons and $GABA_B$ signaling in astrocytes influence memory behaviors including WM (Whissell et al. 2019; Mederos et al. 2021). In human studies, GABA concentration in the occipital cortex, perigenual anterior cingulate and dorsolateral prefrontal cortex has been shown to correlate with changes in WM task accuracy between low and high memory load conditions (Takei et al. 2016; Yoon et al. 2016). In the present study, we found that $GABA_A$ receptor density correlated both with reactions times in the highest load condition as well as with reaction-time differences between high and low load conditions (3- vs. 1-back). These effects were detected in the parietal and prefrontal cortices as well as in the temporo-parietal junction, highlighting that the effect of the GABAergic system on WM performance spans wide cortical networks. Moreover, they demonstrate that properties of the GABAergic system influence multiple aspects of WM task performance. Notably, previous studies have shown that in addition to GABA signaling, the amplitude of oscillatory activity—especially in the beta- and gamma-band—correlates with WM task accuracy (Honkanen et al. 2015; Takei et al. 2016). While we did not replicate these findings, we saw tendencies of this phenomenon in the gamma band for the accuracy, sensitivity, and specificity measures. This suggests the possibility that high-frequency oscillations critically support WM task performance beyond direct inhibitory mechanisms but that the detection of these effects requires a larger cohort of subjects than for the link between WM performance and PET-FMZ-based estimates of $GABA_A$ receptor density. It should also be noted that studies in schizophrenia patients have shown that WM can be influenced in more elaborate manners than just via GABA concentration (Ragland et al. 2020) and that the neuronal architecture of GABAergic inhibitory regulation can vary across cortical regions (Tsubomoto et al. 2019). Thus, to capture the intricacies of the role of GABAergic signaling in WM, $GABA_A$ receptor density measurements should be complemented by other measures that highlight more specific aspects of the GABAergic system.

Although the sample size in this study is an obvious limitation, the data provide a very rare opportunity to examine within the same individuals, data collected using MEG, fMRI, and Flu-PET. Because these unique data sets were collected from healthy

Downloaded from https://academic.oup.com/cercor/advance-article/doi/10.1093/cercor/bhad522/7512628 by Jyvaskyla University user on 17 January 2024

controls as part of a restricted clinical study on schizophrenia, we were not able to get data from more individuals. We acknowledge that our observations will benefit from replication in the future. Nevertheless, we believe that the statistically significant results reported here provide novel findings that can be useful for current discussions within the cognitive and systems neuroscience communities.

## Conclusions

We simultaneously explored $GABA_A$ receptor distributions, electrophysiological and hemodynamic modulations, and task performance in order to advance our understanding of the links between GABAergic inhibition, hemodynamics and oscillatory modulations in higher-order cortical regions, in an attempt to achieve a more holistic view of the neural basis of WM. Our results show that $GABA_A$ receptor density correlated both with high-frequency neural oscillations as well as with modulation of hemodynamic activity in several higher-order regions—demonstrating that the generation and shaping of gamma-band oscillations in higher-order brain regions supporting WM follow inhibitory interneuron-dependent principles similar to those that have been observed in primary sensory regions. We also observed that among the different neural signals, estimates of GABAergic neurotransmission—as proxied by $GABA_A$ receptor density—were the most predictive measure of behavioral variability in WM across subjects. Taken together, our findings provide key systems neuroscience insights into the role of GABAergic inhibition in shaping neural dynamics in higher-order cortical regions and WM performance. This work paves the way for future studies with larger cohorts that could further delineate on a larger scale the links between synaptic neurotransmission, neuronal oscillations, and hemodynamic brain activity in healthy cognition as well as in neurological and psychiatric conditions.

## Acknowledgments

This research was performed within the framework of the LABEX CORTEX (ANR-11-LABX-0042) of Université de Lyon, within the program ANR-11-IDEX-0007. The funders had no role in study design, data collection and analysis, decision to publish, or preparation of the manuscript.

## Authors' contributions

Jan Kujala (Conceptualization, Formal analysis, Funding acquisition, Methodology, Visualization, Writing—original draft, Writing—review & editing), Carolina Ciumas (Formal analysis, Investigation, Methodology, Validation, Writing—original draft, Writing—review & editing), Julien Jung (Conceptualization, Investigation, Supervision, Writing—original draft, Writing—review & editing), Sandrine Bouvard (Formal analysis, Investigation, Methodology, Validation, Writing—original draft, Writing—review & editing), Françoise Lecaignard (Formal analysis, Investigation, Methodology, Validation, Writing—review & editing), Amélie Lothe (Investigation, Methodology, Validation, Writing—review & editing), Romain Bouet (Methodology, Validation, Writing—review & editing), Philippe Ryvlin (Conceptualization, Funding acquisition, Supervision, Writing—original draft, Writing—review & editing), and Karim Jerbi (Conceptualization, Funding acquisition, Methodology, Supervision, Writing—original draft, Writing—review & editing)

## Supplementary material

Supplementary material is available at *Cerebral Cortex* online.

## Funding

This work was supported by Canada Research Chairs Program (950-232368 to K.J.) and a Discovery Grant from the Natural Sciences and Engineering Research Council of Canada (2021-03426 to K.J.), and a Strategic Research Clusters Program from the Fonds de recherche du Quebec—Nature et technologies (FRQNT) (2023-RS6-309472 to K.J).

*Conflict of interest statement*: None declared.

## References

Alekseichuk I, Turi Z, de Lara G, Antal A, Paulus W. Spatial working memory in humans depends on theta and high gamma synchronization in the prefrontal cortex. *Curr Biol*. 2016:26(12):1513–1521.

Baddeley A. Working memory: looking back and looking forward. *Nat Rev Neurosci*. 2003:4(10):829–839.

Balz J, Keil J, Roa Romero Y, Mekle R, Schubert F, Aydin S, Ittermann B, Gallinat J, Senkowski D. GABA concentration in superior temporal sulcus predicts gamma power and perception in the sound-induced flash illusion. *NeuroImage*. 2016:125:724–730.

Bandettini PA. The BOLD plot thickens: sign- and layer-dependent hemodynamic changes with activation. *Neuron*. 2012:76(3):468–469.

Bartos M, Vida I, Jonas P. Synaptic mechanisms of synchronized gamma oscillations in inhibitory interneuron networks. *Nat Rev Neurosci*. 2007:8(1):45–56.

Boy F, Evans CJ, Edden RA, Singh KD, Husain M, Sumner P. Individual differences in subconscious motor control predicted by GABA concentration in SMA. *Curr Biol*. 2010:20(19):1779–1785.

Brunel N, Wang XJ. What determines the frequency of fast network oscillations with irregular neural discharges? I. Synaptic dynamics and excitation-inhibition balance. *J Neurophysiol*. 2003:90(1):415–430.

Carver FW, Rubinstein DY, Gerlich AH, Fradkin SI, Holroyd T, Coppola R. Prefrontal high gamma during a magnetoencephalographic working memory task. *Hum Brain Mapp*. 2019:40(6):1774–1785.

Cohen MX. A better way to define and describe Morlet wavelets for time-frequency analysis. *NeuroImage*. 2019:199:81–86.

Cohen JR, Sreenivasan KK, D'Esposito M. Correspondence between stimulus encoding- and maintenance-related neural processes underlies successful working memory. *Cereb Cortex*. 2014:24(3):593–599.

Cousijn H, Haegens S, Wallis G, Near J, Stokes MG, Harrison PJ, Nobre AC. Resting GABA and glutamate concentrations do not predict visual gamma frequency or amplitude. *Proc Natl Acad Sci U S A*. 2014:111(25):9301–9306.

D'Esposito M, Postle BR, Ballard D, Lease J. Maintenance versus manipulation of information held in working memory: an event-related fMRI study. *Brain Cogn*. 1999:41(1):66–86.

D'Esposito M, Postle BR, Rypma B. Prefrontal cortical contributions to working memory: evidence from event-related fMRI studies. *Exp Brain Res*. 2000:133(1):3–11.

Dale AM, Liu AK, Fischl BR, Buckner RL, Belliveau JW, Lewine JD, Halgren E. Dynamic statistical parametric mapping: combining fMRI and MEG for high-resolution imaging of cortical activity. *Neuron*. 2000:26(1):55–67.

Downloaded from https://academic.oup.com/cercor/advance-article/doi/10.1093/cercor/bhad522/7512628 by Jyvaskyla University user on 17 January 2024

Daume J, Gruber T, Engel AK, Friese U. Phase-amplitude coupling and long-range phase synchronization reveal frontotemporal interactions during visual working memory. *J Neurosci*. 2017:37(2): 313–322.

Delforge J, Pappata S, Millet P, Samson Y, Bendriem B, Jobert A, Crouzel C, Syrota A. Quantification of benzodiazepine receptors in human brain using PET, [11C]flumazenil, and a single-experiment protocol. *J Cereb Blood Flow Metab*. 1995:15(2):284–300.

Delforge J, Spelle L, Bendriem B, Samson Y, Syrota A. Parametric images of benzodiazepine receptor concentration using a partial-saturation injection. *J Cereb Blood Flow Metab*. 1997:17(3):343–355.

Desikan RS, Ségonne F, Fischl B, Quinn BT, Dickerson BC, Blacker D, Buckner RL, Dale AM, Maguire RP, Hyman BT, et al. An automated labeling system for subdividing the human cerebral cortex on MRI scans into gyral based regions of interest. *NeuroImage*. 2006:31(3):968–980.

Diwadkar VA, Carpenter PA, Just MA. Collaborative activity between parietal and dorso-lateral prefrontal cortex in dynamic spatial working memory revealed by fMRI. *NeuroImage*. 2000:12(1):85–99.

Donoghue T, Haller M, Peterson EJ, Varma P, Sebastian P, Gao R, Noto T, Lara AH, Wallis JD, Knight RT, et al. Parameterizing neural power spectra into periodic and aperiodic components. *Nat Neurosci*. 2020:23(12):1655–1665.

Edden RA, Barker PB. Spatial effects in the detection of gamma-aminobutyric acid: improved sensitivity at high fields using inner volume saturation. *Magn Reson Med*. 2007:58(6):1276–1282.

Edden RA, Muthukumaraswamy SD, Freeman TC, Singh KD. Orientation discrimination performance is predicted by GABA concentration and gamma oscillation frequency in human primary visual cortex. *J Neurosci*. 2009:29(50):15721–15726.

Eriksson J, Vogel EK, Lansner A, Bergstrom F, Nyberg L. Neurocognitive architecture of working memory. *Neuron*. 2015:88(1):33–46.

Ester EF, Sprague TC, Serences JT. Parietal and frontal cortex encode stimulus-specific mnemonic representations during visual working memory. *Neuron*. 2015:87(4):893–905.

Fischl B. FreeSurfer. *NeuroImage*. 2012:62(2):774–781.

Gross J, Kujala J, Hämäläinen M, Timmermann L, Schnitzler A, Salmelin R. Dynamic imaging of coherent sources: studying neural interactions in the human brain. *Proc Natl Acad Sci U S A*. 2001:98(2):694–699.

Gross J, Timmermann L, Kujala J, Salmelin R, Schnitzler A. Properties of MEG tomographic maps obtained with spatial filtering. *NeuroImage*. 2003:19(4):1329–1336.

Honkanen R, Rouhinen S, Wang SH, Palva JM, Palva S. Gamma oscillations underlie the maintenance of feature-specific information and the contents of visual working memory. *Cereb Cortex*. 2015:25(10):3788–3801.

Innis RB, al-Tikriti MS, Zoghbi SS, Baldwin RM, Sybirska EH, Laruelle MA, Malison RT, Seibyl JP, Zimmermann RC, Johnson EW. SPECT imaging of the benzodiazepine receptor: feasibility of in vivo potency measurements from stepwise displacement curves. *J Nucl Med*. 1991:32(9):1754–1761.

Johnson EL, Dewar CD, Solbakk AK, Endestad T, Meling TR, Knight RT. Bidirectional frontoparietal oscillatory systems support working memory. *Curr Biol*. 2017:27(12):1829–1835 e4.

Jung J, Williams SR, Sanaei Nezhad F, Lambon Ralph MA. GABA concentrations in the anterior temporal lobe predict human semantic processing. *Sci Rep*. 2017:7(1):15748.

Khursheed F, Tandon N, Tertel K, Pieters TA, Disano MA, Ellmore TM. Frequency-specific electrocorticographic correlates of working memory delay period fMRI activity. *NeuroImage*. 2011:56(3): 1773–1782.

Kolasinski J, Logan JP, Hinson EL, Manners D, Divanbeighi Zand AP, Makin TR, Emir UE, Stagg CJ. A mechanistic link from GABA to cortical architecture and perception. *Curr Biol*. 2017:27(11): 1685–1691 e3.

Kujala J, Jung J, Bouvard S, Lecaignard F, Lothe A, Bouet R, Ciumas C, Ryvlin P, Jerbi K. Gamma oscillations in V1 are correlated with GABAA receptor density: a multi-modal MEG and Flumazenil-PET study. *Sci Rep*. 2015:5(1):16347.

Laaksonen H, Kujala J, Salmelin R. A method for spatiotemporal mapping of event-related modulation of cortical rhythmic activity. *NeuroImage*. 2008:42(1):207–217.

Lara AH, Wallis JD. The role of prefrontal cortex in working memory: a mini review. *Front Syst Neurosci*. 2015:9:173.

Lloyd CM, Richardson MP, Brooks DJ, Al-Chalabi A, Leigh PN. Extramotor involvement in ALS: PET studies with the GABAA ligand [11C]flumazenil. *Brain*. 2000:123(11):2289–2296.

Logothetis NK. What we can do and what we cannot do with fMRI. *Nature*. 2008:453(7197):869–878.

van Loon AM, Knapen T, Scholte HS, St John-Saaltink E, Donner TH, Lamme VA. GABA shapes the dynamics of bistable perception. *Curr Biol*. 2013:23(9):823–827.

Lozano-Soldevilla D, ter Huurne N, Cools R, Jensen O. GABAergic modulation of visual gamma and alpha oscillations and its consequences for working memory performance. *Curr Biol*. 2014:24(24):2878–2887.

Lundqvist M, Rose J, Herman P, Brincat SL, Buschman TJ, Miller EK. Gamma and Beta bursts underlie working memory. *Neuron*. 2016:90(1):152–164.

Marsman A, Mandl RCW, Klomp DWJ, Cahn W, Kahn RS, Luijten PR, Hulshoff Pol HE. Intelligence and brain efficiency: investigating the association between working memory performance, glutamate, and GABA. *Front Psychiatry*. 2017:8:154.

Maziere M, Hantraye P, Prenant C, Sastre J, Comar D. Synthesis of ethyl 8-fluoro-5,6-dihydro-5-[11C]methyl-6-oxo-4H-imidazo [1,5-a] [1,4]benzodiazepine-3-carboxylate (RO 15.1788-11C): a specific radioligand for the in vivo study of central benzodiazepine receptors by positron emission tomography. *Int J Appl Radiat Isot*. 1984:35(10):973–976.

Mederos S, Sanchez-Puelles C, Esparza J, Valero M, Ponomarenko A, Perea G. GABAergic signaling to astrocytes in the prefrontal cortex sustains goal-directed behaviors. *Nat Neurosci*. 2021:24(1): 82–92.

Michels L, Martin E, Klaver P, Edden R, Zelaya F, Lythgoe DJ, Lüchinger R, Brandeis D, O'Gorman RL. Frontal GABA levels change during working memory. *PLoS One*. 2012:7(4):e31933.

Müller Herde A, Benke D, Ralvenius WT, Mu L, Schibli R, Zeilhofer HU, Krämer SD. GABAA receptor subtypes in the mouse brain: regional mapping and diazepam receptor occupancy by in vivo [18F]flumazenil PET. *NeuroImage*. 2017:150:279–291.

Muthukumaraswamy SD, Edden RA, Jones DK, Swettenham JB, Singh KD. Resting GABA concentration predicts peak gamma frequency and fMRI amplitude in response to visual stimulation in humans. *Proc Natl Acad Sci U S A*. 2009:106(20): 8356–8361.

Myers JF, Rosso L, Watson BJ, Wilson SJ, Kalk NJ, Clementi N, Brooks DJ, Nutt DJ, Turkheimer FE, Lingford-Hughes AR. Characterisation of the contribution of the GABA-benzodiazepine alpha1 receptor subtype to [(11)C]Ro15-4513 PET images. *J Cereb Blood Flow Metab*. 2012:32(4):731–744.

Myers NE, Stokes MG, Nobre AC. Prioritizing information during working memory: beyond sustained internal attention. *Trends Cogn Sci*. 2017:21(6):449–461.

Downloaded from https://academic.oup.com/cercor/advance-article/doi/10.1093/cercor/bhad522/7512628 by Jyvaskyla University user on 17 January 2024

Northoff G, Walter M, Schulte RF, Beck J, Dydak U, Henning A, Boeker H, Grimm S, Boesiger P. GABA concentrations in the human anterior cingulate cortex predict negative BOLD responses in fMRI. *Nat Neurosci*. 2007:10(12):1515–1517.

Oostenveld R, Fries P, Maris E, Schoffelen JM. FieldTrip: open source software for advanced analysis of MEG, EEG, and invasive electrophysiological data. *Comput Intell Neurosci* 2011:2011:156869, 1, 9.

Owen AM, McMillan KM, Laird AR, Bullmore E. N-back working memory paradigm: a meta-analysis of normative functional neuroimaging studies. *Hum Brain Mapp*. 2005:25(1):46–59.

Palva JM, Monto S, Kulashekhar S, Palva S. Neuronal synchrony reveals working memory networks and predicts individual memory capacity. *Proc Natl Acad Sci U S A*. 2010:107(16):7580–7585.

Palva S, Kulashekhar S, Hämäläinen M, Palva JM. Localization of cortical phase and amplitude dynamics during visual working memory encoding and retention. *J Neurosci*. 2011:31(13):5013–5025.

Popov T, Jensen O, Schoffelen JM. Dorsal and ventral cortices are coupled by cross-frequency interactions during working memory. *NeuroImage*. 2018:178:277–286.

Ragland JD, Maddock RJ, Hurtado MY, Tanase C, Lesh TA, Niendam TA, Carter CS, Ranganath C. Disrupted GABAergic facilitation of working memory performance in people with schizophrenia. *Neuroimage Clin*. 2020:25:102127.

Rahm B, Kaiser J, Unterrainer JM, Simon J, Bledowski C. fMRI characterization of visual working memory recognition. *NeuroImage*. 2013:90C:413–422.

Rodermund P, Westendorff S, Nieder A. Blockage of NMDA- and GABA(A) receptors improves working memory selectivity of primate prefrontal neurons. *J Neurosci*. 2020:40(7):1527–1537.

Roux F, Uhlhaas PJ. Working memory and neural oscillations: alpha-gamma versus theta-gamma codes for distinct WM information? *Trends Cogn Sci*. 2014:18(1):16–25.

Roux F, Wibral M, Mohr HM, Singer W, Uhlhaas PJ. Gamma-band activity in human prefrontal cortex codes for the number of relevant items maintained in working memory. *J Neurosci*. 2012:32(36):12411–12420.

Salmi E, Aalto S, Hirvonen J, Långsjö JW, Maksimow AT, Oikonen V, Metsähonkala L, Virkkala J, Någren K, Scheinin H. Measurement of GABAA receptor binding in vivo with [11C]flumazenil: a test-retest study in healthy subjects. *NeuroImage*. 2008:41(2):260–269.

Schmidt-Wilcke T, Fuchs E, Funke K, Vlachos A, Müller-Dahlhaus F, Puts NAJ, Harris RE, Edden RAE. GABA—from inhibition to cognition: emerging concepts. *Neuroscientist*. 2018:24(5):501–515.

Soreq E, Leech R, Hampshire A. Dynamic network coding of working-memory domains and working-memory processes. *Nat Commun*. 2019:10(1):936.

Stokes PR, Myers JF, Kalk NJ, Watson BJ, Erritzoe D, Wilson SJ, Cunningham VJ, Barros DR, Hammers A, Turkheimer FE, et al. Acute increases in synaptic GABA detectable in the living human brain: a [11C]Ro15-4513 PET study. *NeuroImage*. 2014:99:158–165.

Sumner P, Edden RA, Bompas A, Evans CJ, Singh KD. More GABA, less distraction: a neurochemical predictor of motor decision speed. *Nat Neurosci*. 2010:13(7):825–827.

Takei Y, Fujihara K, Tagawa M, Hironaga N, Near J, Kasagi M, Takahashi Y, Motegi T, Suzuki Y, Aoyama Y, et al. The inhibition/excitation ratio related to task-induced oscillatory modulations during a working memory task: a multtimodal-imaging study using MEG and MRS. *NeuroImage*. 2016:128:302–315.

Terhune DB, Russo S, Near J, Stagg CJ, Cohen KR. GABA predicts time perception. *J Neurosci*. 2014:34(12):4364–4370.

Tsubomoto M, Kawabata R, Zhu X, Minabe Y, Chen K, Lewis DA, Hashimoto T. Expression of transcripts selective for GABA neuron subpopulations across the cortical visuospatial working memory network in the healthy state and schizophrenia. *Cereb Cortex*. 2019:29(8):3540–3550.

van de Ven V, Jacobs C, Sack AT. Topographic contribution of early visual cortex to short-term memory consolidation: a transcranial magnetic stimulation study. *J Neurosci*. 2012:32(1):4–11.

Wang M, Yang Y, Wang CJ, Gamo NJ, Jin LE, Mazer JA, Morrison JH, Wang XJ, Arnsten AFT. NMDA receptors subserve persistent neuronal firing during working memory in dorsolateral prefrontal cortex. *Neuron*. 2013:77(4):736–749.

Whissell PD, Bang JY, Khan I, Xie YF, Parfitt GM, Grenon M, Plummer NW, Jensen P, Bonin RP, Kim JC. Selective activation of cholecystokinin-expressing GABA (CCK-GABA) neurons enhances memory and cognition. *eNeuro*. 2019:6(1):ENEURO.0360–ENEU18.2019.

Whittington MA, Traub RD. Interneuron diversity series: inhibitory interneurons and network oscillations in vitro. *Trends Neurosci*. 2003:26(12):676–682.

Yoon JH, Maddock RJ, Rokem A, Silver MA, Minzenberg MJ, Ragland JD, Carter CS. GABA concentration is reduced in visual cortex in schizophrenia and correlates with orientation-specific surround suppression. *J Neurosci*. 2010:30(10):3777–3781.

Yoon JH, Grandelis A, Maddock RJ. Dorsolateral prefrontal cortex GABA concentration in humans predicts working memory load processing capacity. *J Neurosci*. 2016:36(46):11788–11794.

Downloaded from https://academic.oup.com/cercor/advance-article/doi/10.1093/cercor/bhad522/7512628 by Jyvaskyla University user on 17 January 2024